Electronic Supplementary Material (ESI) for Nanoscale.

Supplementary Information

Effect of Topography on Wetting of Nanoscale Patterns: Experimental and Modeling Studies

*Harpreet S. Grewal, Il-Joo Cho, Jae-Eung Oh , Eui-Sung Yoon**

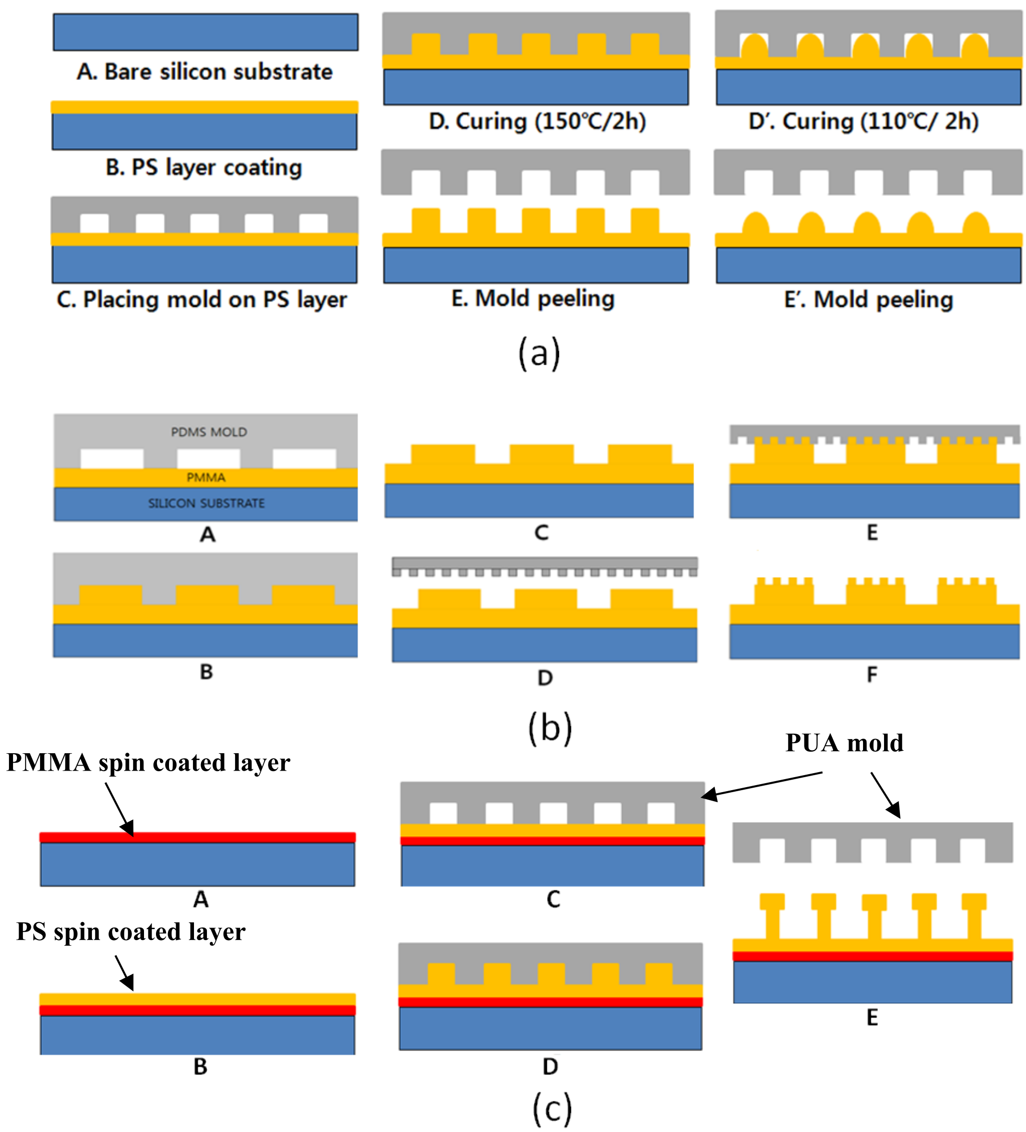

Figure S1: Schematic illustrating the fabrication procedure used for the obtaining (a) Pillar (b) Hierarchical and (c) Mushroom patterns. Pillar shape patterns were prepared using capillary force lithography technique. Use of different curing temperatures resulted in cylindrical and dome shaped pillar patterns. Similarly the change in curing temperature helped in developing Mushroom patterns with flat and round tops

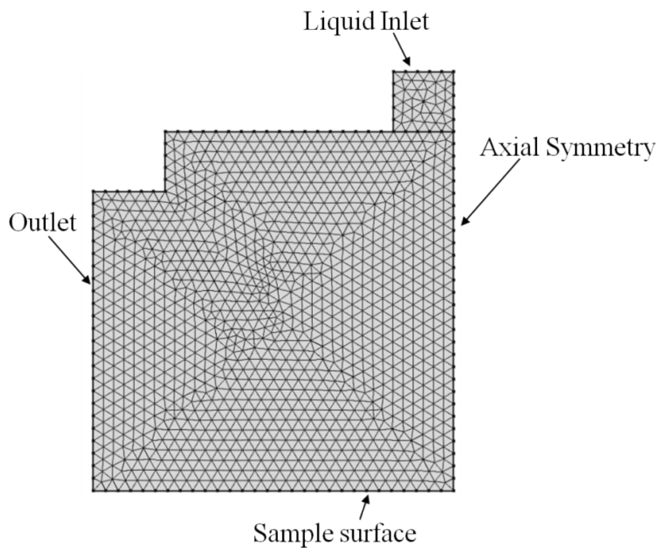

Figure S2: The meshed domain used for modeling the liquid droplet simulations. The boundary condition used are also marked

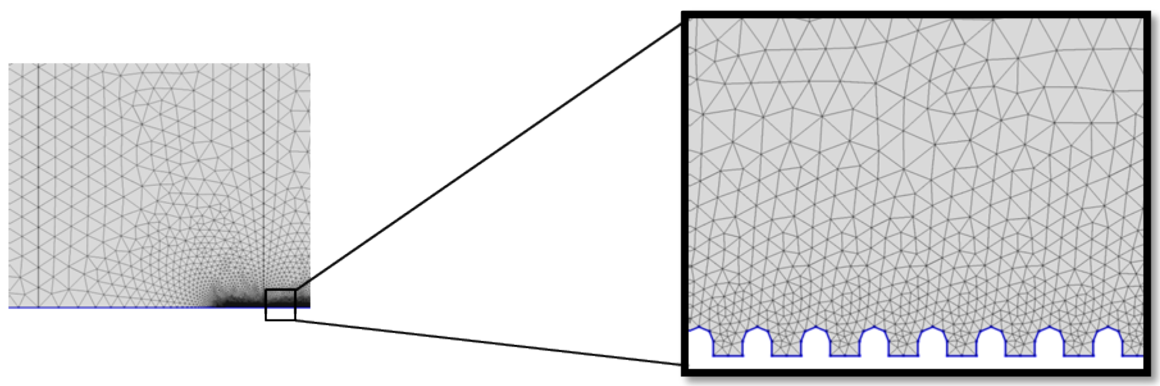

(a)

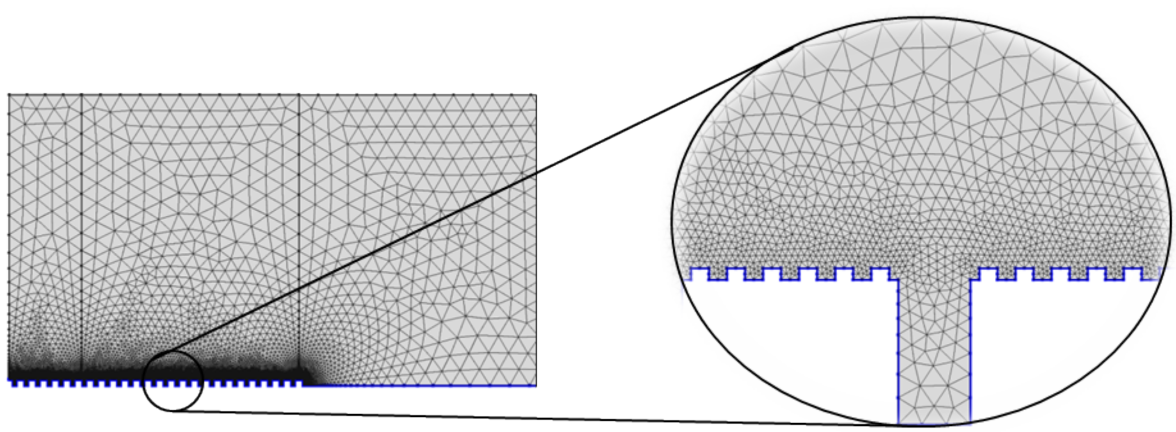

(b)

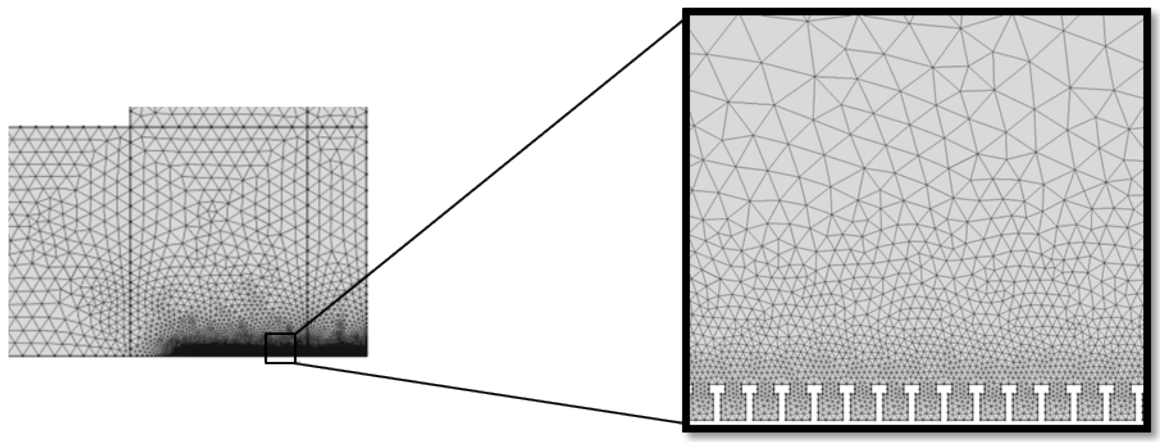

(c)

Figure S3: The meshed domains for (a) dome (b) hierarchical and (c) mushroom shape patterns.

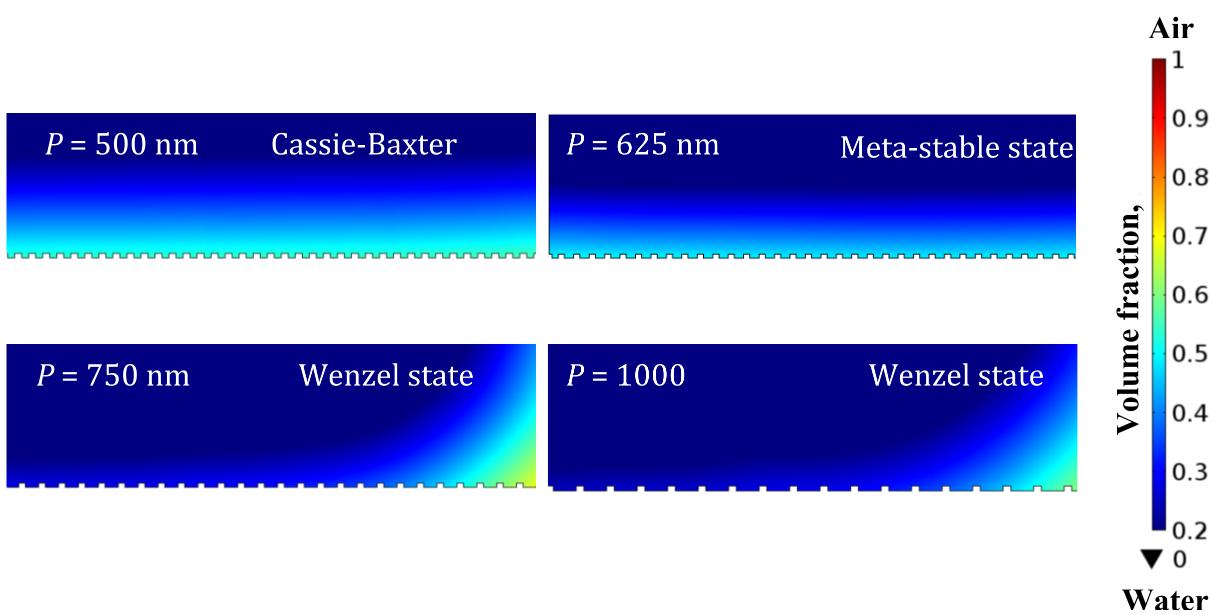

Figure S4: Volume fraction plots obtained from FEM simulations for cylindrical patterns showing the transition in wettability state from Cassie-Baxter to Wenzel with increasing pitch, P (not to scale). The sky blue line corresponds to $\phi = 0.5$ marks the boundary between the water and air as shown in attached color bar.

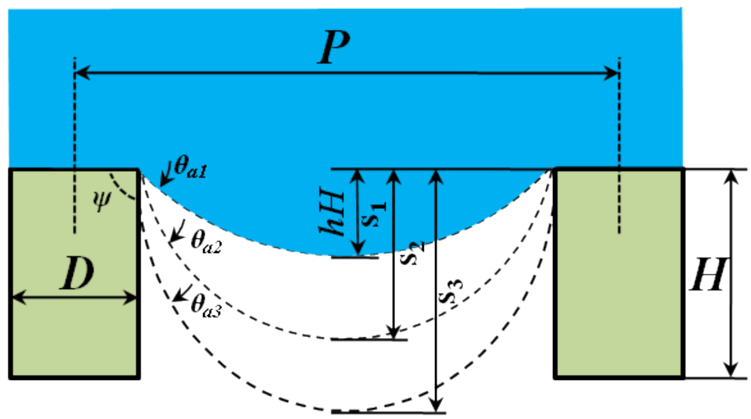

Figure S5: Schematic illustration of different geometric parameters and sagging depths (s_1, s_2, s_3) for three cases. The sagging depth $\left(D\left(\sqrt{2}S_f-1\right)\tan\left(\theta_a-\psi\right)/2\right)$ is different from the penetration depth (*hH*) and can be greater than the height (*H*) of the pattern, mathematically.

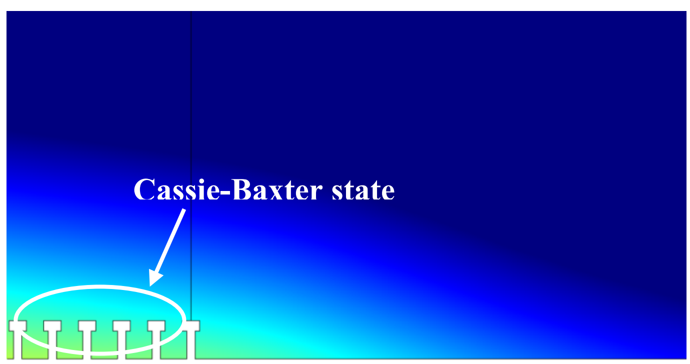

(a)

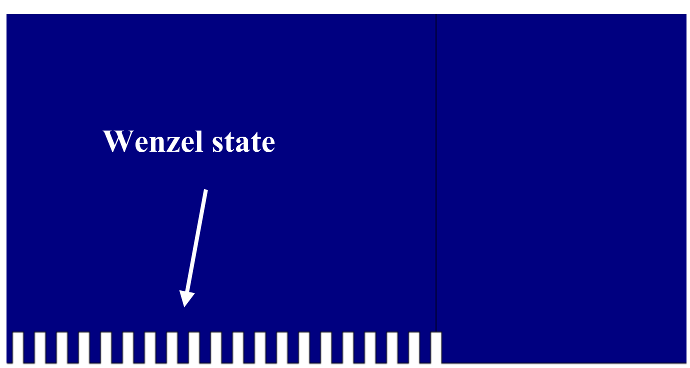

(b)

Figure S6: Comparison of the capability of the (a) mushroom and (b) cylindrical patterns in sustaining the air and hence the Cassie-Baxter state. It can be observed that among the topography shapes both with PS surface and geometry parameters (pitch=500 nm, height =550 nm), mushroom shape pattern is highly effective in restraining a layer of air and sustaining the Cassie-Baxter state. However, cylindrical shape could not effectively restrain the Cassie-Baxter state and gets transform into Wenzel state. This highlights the importance of topography shape in withholding the Cassie-Baxter state.

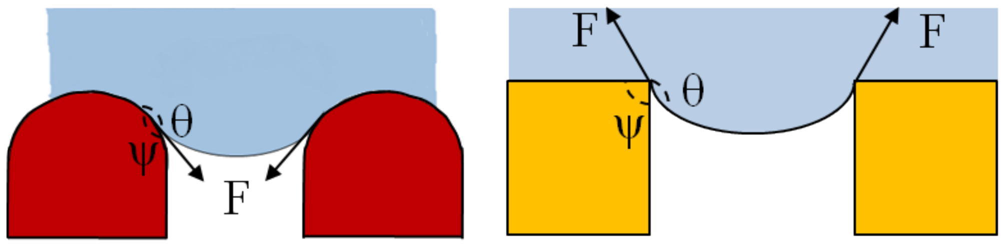

Figure S7: Schematic illustrating geometric angle ψ and the direction of force depending upon contact angle θ after Tuteja [7].

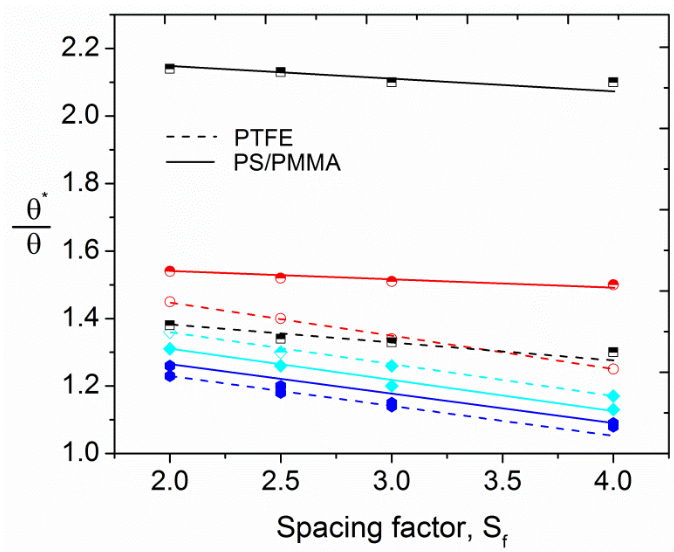

Figure S8: Correlation between spacing factor, S_f and cosine of contact angle (θ^*) for patterned surface normalized by the cosine of the contact angle (θ) of the flat surface for (⬢) Dome (◆) Cylinder (●) Mushroom and (■) Hierarchical patterns. Filled symbols represent Wenzel state wetting state, semi-filled the meta-stable state and open ones represents the Cassie-Baxter state.

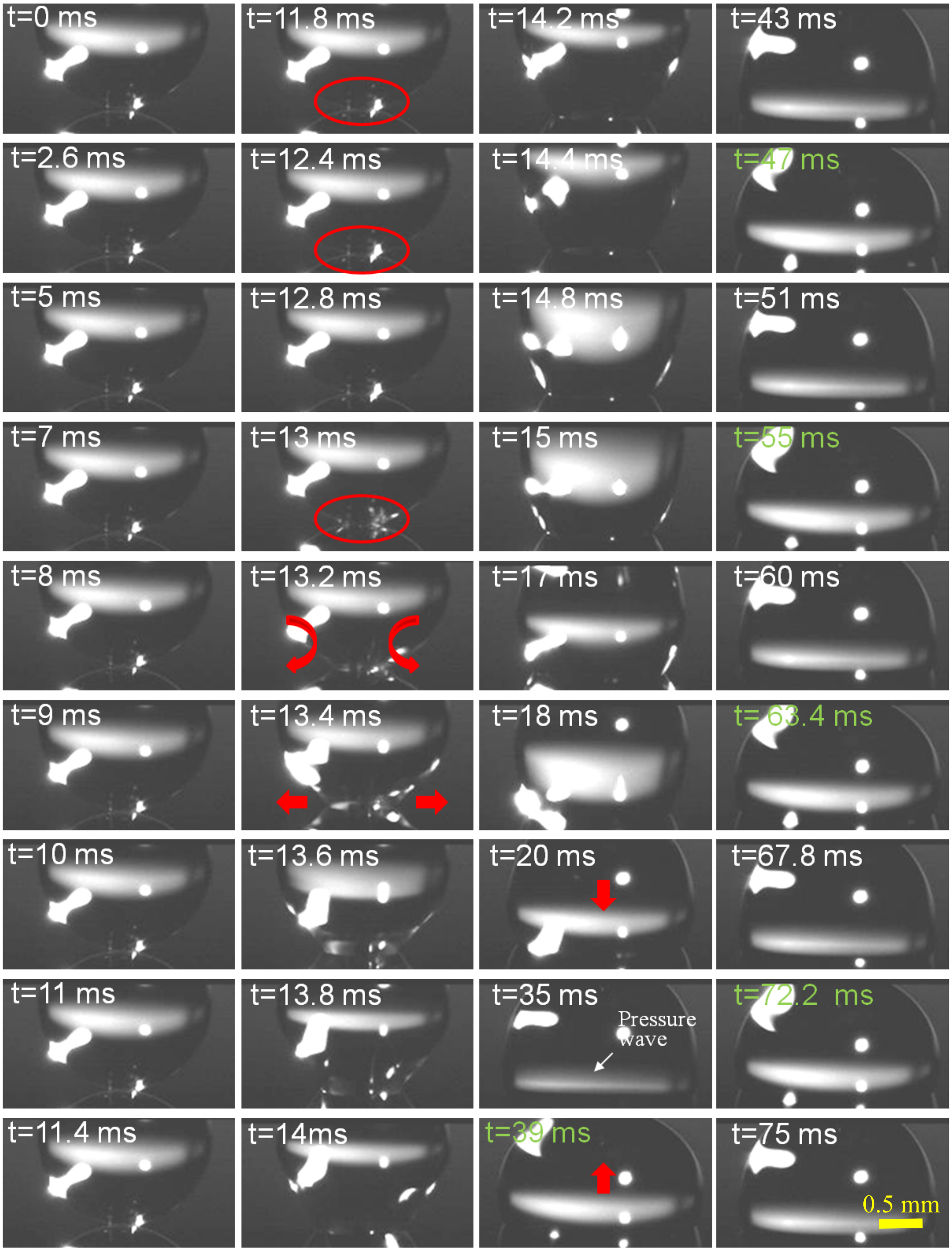

Figure S9: High speed imaging showing the interaction between the water droplet held at static position and polystyrene (PS) surface. The images were captured at 5000 frames per second with shutter speed of 0.0001 s.

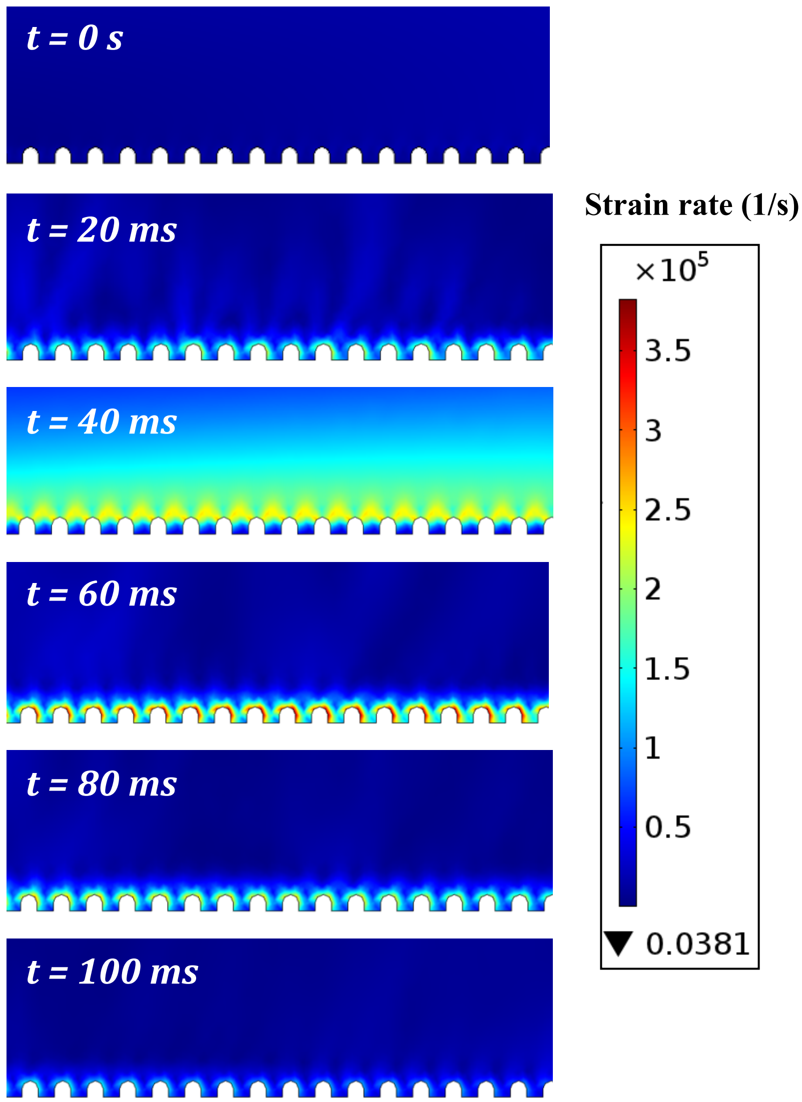

t = 0 s
t = 20 ms
t = 40 ms
t = 60 ms
t = 80 ms
t = 100 ms
Strain rate (1/s)
×10^5
3.5
3
2.5
2
1.5
1
0.5
0.0381

(a)

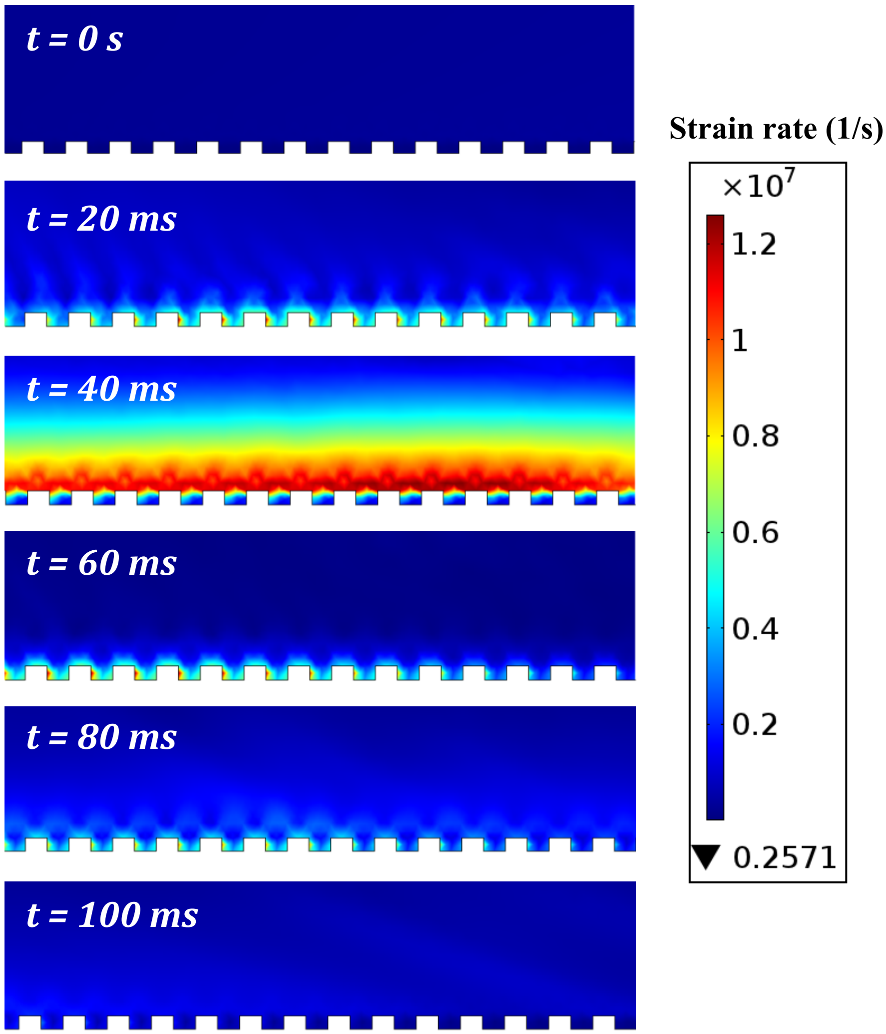

(b)

Figure S10: The plots showing the variation in strain rates for (a) dome and (b) cylindrical patterns with time. The magnitude of strain rates for respective plot is represented by adjacent color scale.

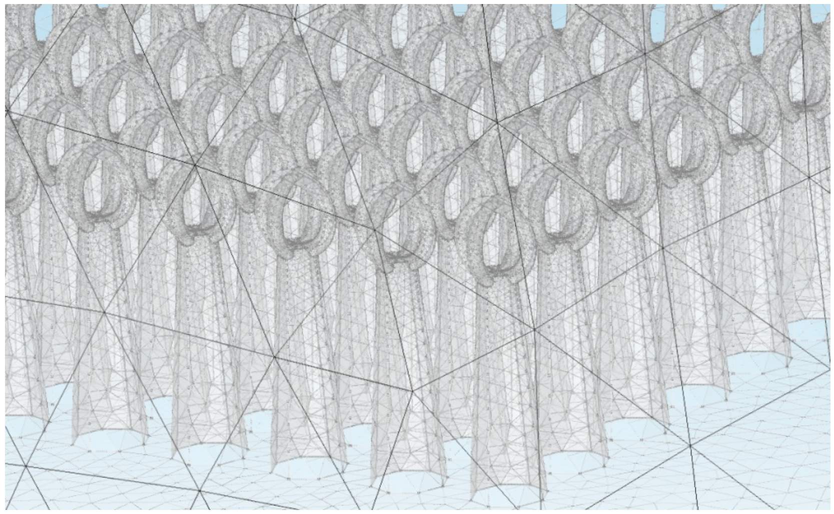

Figure S11: The meshed model of Salvinia Molesta leaf used for FEM simulations

Table S1: The various topographical shapes and their surface materials and geometric dimensions investigated in present work. Here, *D, P* and *H* represents the diameter, pitch and the height of the patterns

Shape		Micrograph	Dimensions (nm)						Material		
			D	P				H	PS	PMMA	PTFE
				500	625	750	1000				
Dome		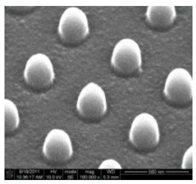	250	●	●	●	●	250	●		●
Cylinder		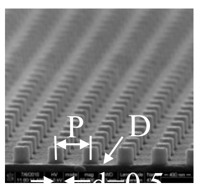	250	●	●	●	●	250	●		●
Mushroom		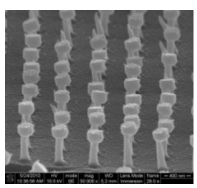	250	●	●	●	●	550	●		●
Mushroom		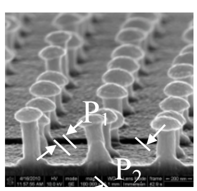	250	●				550	●		●
Hierar--chical	Nano part	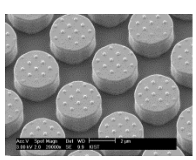	250	●	●	●	●	160		●	●
Hierar--chical	Micro part		3 µm	P_2 = 4 µm				2 µm		●	●

Table S2: The comparison of the wettability states predicted by different approaches. The filled and open symbols represent the Wenzel and Cassie-Baxter states, respectively. Whereas, the half-filled symbols represent the meta-stable states. The color of the symbols represents the syrface of the patterns with red used for polystyrene (PS), yellow for polymethylmethacrylate (PMMA) and green color for the patterns with polytetrafluoroethylene (PTFE) surface.

Pattern	**Pitch (nm)**	**Quere's Model (Eq 1)**		**Gibb's free energy model**		**FEM simulations**	
Dome	500	●	○	●	●	●	●
	625	●	●	●	●	●	●
	750	●	●	●	●	●	●
	1000	●	●	●	●	●	●
Cylinder	500	●	○	●	○	●	○
	625	●	○	●	◐	●	◐
	750	●	●	●	●	●	●
	1000	●	●	●	●	●	●
Mushroom	500	○	○	○	○	○	○
	625	○	○	○	○	○	○
	750	●	○	◐	○	◐	○
	1000	●	○	◐	○	◐	○
Mushroom with round top	500	○	○	◐	◐	◐	◐
Hierarchical	500	○	○	◐	●	◐	◐
	625	○	○	◐	●	◐	◐
	750	○	○	◐	●	◐	◐
	1000	○	○	◐	●	◐	◐

Table S3: The wettability models used for predicting the contact angles for the patterns surfaces. The comparison of the results predicted by these models with the experimental results is shown in figure 8.

Model	**Expression**	**Remarks**	**Reference**
Wenzel	$\cos\theta_w = r\cos\theta$	r is roughness factor	Wenzel [13]
Cassie-Baxter	$\cos\theta_{C-B} = f_s(\cos\theta+1)-1$	f_s is solid fraction	Cassie and Baxter [14]
Modified Wenzel	$\cos\theta_{mW} = r\cos\theta-\left(1-f_s\right)(\mathrm{r}\cos\theta+1)$		Bhushan and Jung [2]
Modified Cassie-Baxter	$\cos\theta_{mC-B} = f_s(\mathrm{r}\cos\theta+1)-1$		Choi et al [23]
Dual roughness with Cassie (m)-Cassie (n)	$\cos\theta^{C-C} = f_n f_m(\cos\theta+1)-1$	f – solid fraction m – microscale n- nanoscale	Rahmawan et al [20]
Dual roughness with Wenzel (m)-Cassie (n)	$\cos\theta^{W-C} = r_m\left(f_n(\cos\theta+1)-1\right)$		
Dual roughness with Cassie (m)-Wenzel (n)	$\cos\theta^{C-W} = r_n\left(f_m(\cos\theta+1)-1\right)$		
Dual roughness with Wenzel (m)-Wenzel (n)	$\cos\theta^{W-W} = r_n r_m\cos\theta$		